Gene Expression Analysis of So Called Asian Dust Extracts in Human Acute Myeloid Leukemia Cells

You-Jin Choi[1], Hu-Quan Yin[1], Eun-Jung Park[2], Kwangsik Park[2], Dae-Seon Kim[3] and Byung-Hoon Lee[1]

[1]*College of Pharmacy and Research Institute of Pharmaceutical Sciences, Seoul National University, Seoul 151-742*
[2]*College of Pharmacy, Dongduk Women's University, Seoul 136-714*
[3]*Department of Environmental Health and Safety, National Institute of Environmental Research, Incheon 404-170, Korea*

As the frequency and the intensity of so called Asian dust (AD) events have increased, public concerns about the adverse health effects has spiked sharply over the last two decades. Despite the recent reports on the correlation between AD events and the risk for cardiovascular and respiratory disease, the nature of the toxicity and the degree of the risk are yet largely unknown. In the present study, we investigated the effects of the dichloromethane extract of AD (AD-X) and that of urban dust (NAD-X) collected during a non-AD period on gene expression in HL-60 cells using Illumina Sentrix HumanRef-8 Expression BeadChips. Global changes in gene expression were analyzed after 24 h of incubation with 50 or 100 μg/m*l* AD-X and NAD-X. By one-way analysis of variance ($p < 0.05$) and Benjamini-Hochberg multiple testing correction for false discovery rate of the results, 573 and 297 genes were identified as AD-X- and NAD-X-responsive, respectively. The genes were classified into three groups by Venn diagram analysis of their expression profile, i.e., 290 AD-X-specific, 14 NAD-X-specific, and 283 overlapping genes. Quantitative real-time PCR confirmed the changes in the expression levels of the selected genes. The expression patterns of five genes, namely *SORL1*, *RABEPK*, *DDIT4*, *AZU1*, and *NUDT1* differed significantly between the two groups. Following rigorous validation process, these genes may provide information in developing biomarker for AD exposure.

Key words: Air pollution, Asian dust, Biomarker, HL-60 cells, Microarray, Biomarker

INTRODUCTION

Asian dust (AD), or yellow sand, is a seasonal meteorological phenomenon that originates during springtime in the arid deserts of Mongolia and China. Although AD primarily affects the East Asian region, including China, Korea, and Taiwan, analyses of atmospheric particles reveal that a considerable amount of AD is transported to Hawaii and the western coast of North America (Parrington *et al.*, 1983; Husar *et al.*, 2001). AD events have a long history. We also have records of AD in the ancient history of Korea containing keywords that include "sand rain," "red snow," and "severe dust fall." However, the problem is that the number of days of AD events observed in the cities of East Asia has increased dramatically in the last 20 years due to accelerating desertification by overgrazing and overfarming in the

central and western regions of Inner Mongolia (Chun *et al.*, 2003).

Silicon, aluminum, sulfur, calcium, and titanium are the major trace elements that increase during AD events in Korea (Han *et al.*, 2004). In addition to the mineral composition of the particles themselves, dust can carry with it a variety of chemical contaminants that are adsorbed to the particulate matter during the long-distance transport through heavily industrialized eastern China (Taylor, 2002). They include persistent organic pollutants and heavy metals, which may adversely affect human health and the environment (Park *et al.*, 2008). Adverse health effects caused by exposure to AD have been reported in many epidemiologic studies. Kwon *et al.* (2002) demonstrated a strong correlation between AD events and death from cardiovascular and respiratory causes. Similar results were reported in Taiwan: cardiopulmonary emergency visits increased due to AD transported over long distances (Chan *et al.*, 2008).

Due to many factors contributing to the adverse health effects of AD, such as the complexity in chemical composition and the effects of the particles per se, a full understand-

Correspondence to: Byung-Hoon Lee, College of Pharmacy, Seoul National University, San 56-1, Sillim-dong, Gwanak-gu, Seoul 151-742, Korea
E-mail: lee@snu.ac.kr

ing of the nature of the toxicity and the degree of the risk of AD is difficult. Unresolved but critical components of risk assessment of AD include the development of biomarkers for the evaluation of exposure. The identification of differentially expressed genes or patterns of gene expression using a microarray hybridization assay provides a logical approach to studying the detailed mechanisms of toxicity as well as to identifying potential biomarkers of toxicity (Li *et al.*, 2007). Many studies have suggested the use of gene biomarkers for the diagnosis and prognosis of disease, as well as for the assessment of exposure to xenobiotics in cells and tissues (Forrest *et al.*, 2005; Mohr and Liew, 2007). To this end, we investigated the effects of AD on gene expression in human myeloid leukemia cells. The goals of the present study were to screen gene expression profiles and to identify candidate gene markers for the inference of toxicity.

MATERIALS AND METHODS

Cells and materials. The human promyelocytic leukemia cells (HL-60, ATCC CCL-240) were maintained in RPMI-1640 with L-glutamine, 25 mM HEPES and 25 mM $NaHCO_3$ supplemented with 10% fetal bovine serum (FBS) and 1% antibiotic-antimycotics (penicillin, streptomycin and amphotericin B) in a 5% CO_2 atmosphere at 37°C. RPMI-1640, FBS and antibiotic-antimycotics were purchased from Gibco (Grand Island, NY).

Collection of Asian dust was performed using high volume TSP sampler (Tisch Environmental, TE-5200, USA) at the northern part of Seoul. AD was collected at May 8, 13, 25 and 26, 2007, when official reports of AD storm were released by the national weather agency. NAD was collected between July 10 and 18, when no AD event was reported. The average concentration of Particulate Matter10 (PM_{10}) during AD sample collection was 139.72 µg/m³, while that of PM_{10} during NAD sample collection was 19.77 µg/m³. The same amounts of the total suspended particle samples were sonicated in dichloromethane (200 m*l*) three times with mild warming, and then the extract was evaporated. The dichloromethane extract of AD (AD-X) and that of

NAD (NAD-X) were resolubilized in DMSO and filtered for the microarray assay.

Cell viability measurement. Cells were seeded with 5×10^4 cells per well in 96 well plates and incubated for 3 h. After incubation with AD-X or NAD-X for 24 h with various concentrations (0, 1, 10, 50, 100 and 200 µg/m*l*), cell viability was measured using the 3-(4,5-dimethylthia-zol-2-yl)-2,5-diphenyltetrazolium bromide (MTT) cell proliferation assay.

Microarray hybridization. Cells were exposed to AD-X or NAD-X (0, 50 and 100 µg/ml) for 24 h and total RNA was extracted using an Easy-Blue™ total RNA extraction kit (Intron Biotech, Sungnam, Korea). Sentrix HumanRef-8 Expression Bead Chips (Illumina, San Diego, CA) containing more than 24,000 genes were used to analyze differential gene expression profiles. A detailed description of the BeadChip system has been provided elsewhere (Kuhn *et al.*, 2004). Briefly, biotinylated cRNA was prepared and linearly amplified from 0.5 µg of total RNA using an Illumina RNA Amplification kit (Ambion, Austin, TX) and purified using the Qiagen RNeasy kit (Qiagen, Basel, Switzerland). Hybridization, washing and scanning were performed using Illumina Bead Station 500× and Illumina Bead Array Reader Confocal Scanner. The quality of hybridization and overall chip performance were monitored by visual inspection of both internal quality control checks and the raw scanned data. Raw data were extracted using the software BeadStudio (v. 3.1.0). Array data were filtered by detection $p < 0.05$ (similar to signal to noise) in at least 50% samples. Selected gene signal value was transformed by logarithm and normalized by quantile method.

Data analysis. The comparative analysis of samples was carried out using one-way analysis of variance (ANOVA). Since the ANOVA test is repeated for each gene, we did Benjamini-Hochberg multiple-testing correction for false discovery rate control of the results ($p < 0.05$). Hierarchical cluster analysis was performed using complete linkage and

Table 1. Gene specific primers used in quantitative real-time PCR

| Gene	NCBI RefSeq	Forward primer (5'-3')	Reverse primer (5'-3')
AZU1	NM_001700.3	5' GTGGTGCTGGGTGCCTATGAC 3'	5' CACGCTGCTGGTGAGGTTGG 3'
RP11-529I10.4	NM_015448.1	5' AAGGAAAGCAATGCCAATC 3'	5' AGGCGTCATCCAGAGGTAG 3'
NUDT1	NM_198954.1	5' GGCTCTATACCCTGGTGCTG 3'	5' TCCTGACCCTGGAACTTGA 3'
RABEPK	NM_005833.2	5' CTGACCGTATCTGGGTATTT 3'	5' CTGCCATTTCATGTCACTTAT 3'
ARMET	NM_006010.2	5' TACCAGGACCTCAAAGACAG 3'	5' GGGCATATTTAGGCATCAGT 3'
FLJ10081	NM_017991.3	5' CGCAGCGTGATGAATGAGT 3'	5' GCAGATGGGTGGCTACAGG 3'
CSTB	NM_000100.2	5' GTTTAAGGCCGTGTCATTC 3'	5' CTTGGCTTTGTTGGTCTGG 3'
CD55	NM_000574.2	5' AAATCATGCCCTAATCCG 3'	5' CTGCCTGAAATAAGACAAA 3'
DDIT4	NM_019058.2	5' CTCTTCGCCCTCGTCCTT 3'	5' AGCCAGTGCTCAGCGTCA 3'
GAPDH	NM_002046.3	5' AACGGATTTGGTCGTATTG 3'	5' GCTCCTGGAAGATGGTGAT 3'

Euclidean distance as a measure of similarity. All data analysis and visualization of differentially expressed genes was conducted using ArrayAssist® (Stratagene, La Jolla, CA) and R (ver. 2.5; http://www.r-project.org). Biological pathway and ontology-based analysis were performed by using Panther database (http://www.pantherdb.org).

Quantitative real-time reverse transcriptase polymerase chain reaction. Total RNA was purified using the Easy-Blue™ Total RNA Extraction Kit (Intron Biotech, Korea) and then used to synthesize single-strand cDNA using Superscript™ III First-Strand Synthesis System for RT-PCR (Invitrogen, Carlsbad, CA). Gene-specific primers (Table 1) were designed using Primer Premier (Premier Biosoft International, Palo Alto, CA). Quantitative realtime RT-PCR (Q-PCR) was performed using a Fast Start DNA Master SYBR Green I Mixture kit (Roche Diagnostics, USA) in a Light Cycler system (Roche Diagnostics, USA) according to the manufacturer's protocol. To confirm the specificity of amplification, melting curve analysis was applied to all final PCR products.

RESULTS

Cytotoxicity of AD-X and NAD-X. To establish the optimal concentration of the test samples for microarray hybridization analysis, we incubated HL-60 cells with media containing 0~200 μg/ml AD-X and NAD-X for 24 h and then determined cell viability using the MTT colorimetric assay. The concentrations of AD-X and NAD-X that induced the half-maximal cytotoxic effects were 120.5 ± 10.9 and 149.6 ± 13.3 μg/ml, respectively (Fig. 1).

Identification of specific AD-X- and NAD-X-responsive genes. On the basis of the data obtained in the cytotoxicity assay, global changes in gene expression were analyzed
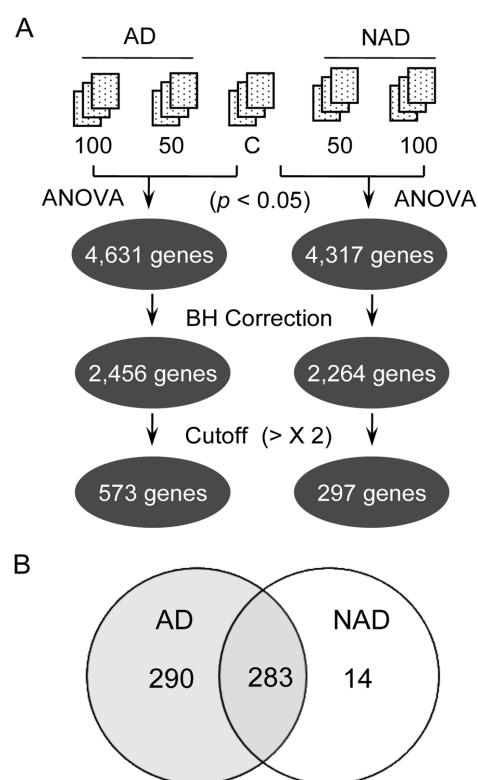
Fig. 2. Flowchart for data analysis and Venn diagram analysis. (A) The microarray data were analyzed by one-way ANOVA, adjusted by the Benjamini-Hochberg multiple testing correction, and subjected to a cutoff of twofold or greater induction or repression. AD and NAD indicate Asian dust and non-Asian dust, respectively, and the numbers after the symbol indicate the dose of the sample in mg/ml. (B) Venn diagram analysis was performed with data obtained from the analysis as described in Fig. 2A. Numbers in each complete circle denote the total numbers of up- and downregulated genes to the indicated treatment; those in the overlapping region depict the number of shared genes between the two treatment conditions.
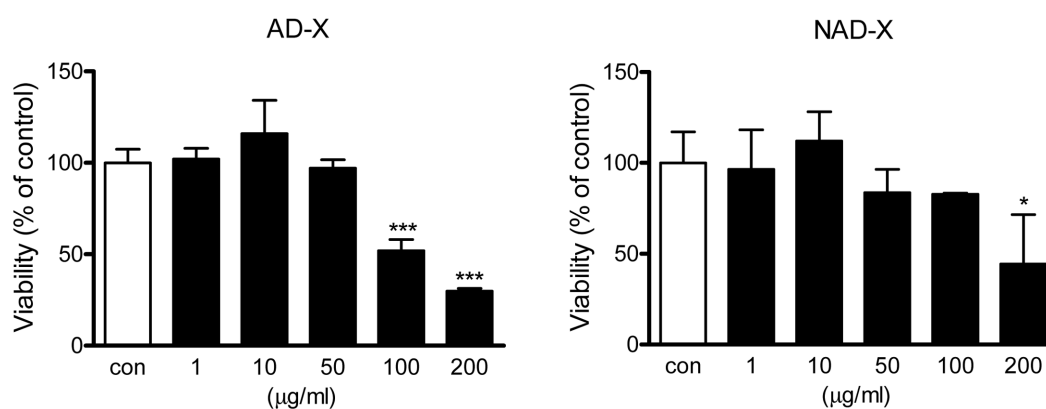
Fig. 1. Acute cytotoxicity of AD-X and NAD-X in human promyelocytic leukemia cells (HL-60). The cells were incubated with increasing concentrations of AD-X or NAD-X in media containing 10% fetal bovine serum for 24 h, after which viability was determined by MTT assay. Results are expressed as the percentage of viable cells compared to solvent controls.

Table 2. Top 10 up- and down-regulated genes (one-way ANOVA; $p < 0.05$) compared with control in the HL-60 cells treated with AD-X

NCBI ref	Gene symbol	p-value	Fold change AD50	Fold change AD100	Panther Process
NM_002777.3	PRTN3	0.01	−1.99	−6.51	PM
NM_152851.1	MS4A6A (transcript variant 3)	0.01	−3.14	−4.23	unclassified
NM_022349.2	MS4A6A (transcript variant 2)	0.01	−3.52	−4.01	unclassified
NM_005218.3	DEFB1	0.01	−2.03	−3.68	ID
NM_001972.2	ELA2	0.01	−0.98	−3.19	PM; ID
NM_020070.2	IGLL1	0.01	−1.31	−3.04	ID
NM_001700.3	AZU1	0.01	−1.18	−3.02	PM
NM_000647.3	CCR2	0.01	−2.46	−2.94	ST; ID; CS
NM_004772.1	C5orf13	0.01	−2.14	−2.80	unclassified
NM_003039.1	SLC2A5	0.01	−0.69	−2.75	CM; T
NM_000903.2	NQO1	0.01	2.44	3.80	unclassified
NM_005980.2	S100P	0.01	2.36	3.92	unclassified
NM_052815.1	IER3	0.01	0.79	3.92	ID
NM_000265.1	NCF1	0.01	1.80	3.99	ET; ST
NM_001423.1	EMP1	0.01	0.42	4.21	AP; DP; CC; CP; O
NM_000584.2	IL8	0.01	3.14	4.28	ST; ID; DP; CP; CS
NM_015991.1	C1QA	0.01	3.78	4.31	ID
NM_000576.2	IL1B	0.01	1.41	4.43	ST; ID; AP; CC; CP
NM_000591.1	CD14	0.01	1.09	4.81	ID
NM_002982.3	CCL2	0.01	2.18	4.93	ST; ID

Values represent fold changes on $\log_2$ scale compared with control groups. AP, Apoptosis; CC, Cell cycle; CM, Carbohydrate metabolism; CP, Cell proliferation and differentiation; CS, Cell structure and motility; DP, Developmental processes; ET, Electron Transport; ID, Immunity and defense; O, Oncogenesis; PM, Protein metabolism & modification; ST, Signal transduction; T, Transport.

Table 3. Top 10 up- and down-regulated genes (one-way ANOVA; $p < 0.05$) compared with control in the HL-60 cells treated with NAD-X

NCBI ref	Gene symbol	p-value	Fold change NAD50	Fold change NAD100	Panther Process
NM_002777.3	PRTN3	0.01	−1.61	−4.47	PM
NM_152851.1	MS4A6A (transcript variant 3)	0.01	−3.04	−4.00	unclassified
NM_022349.2	MS4A6A (transcript variant 2)	0.01	−3.31	−3.93	unclassified
NM_020070.2	IGLL1	0.01	−1.18	−3.42	ID
NM_005218.3	DEFB1	0.01	−1.76	−3.28	ID
NM_000647.3	CCR2	0.01	−2.33	−2.74	ST; ID; CS
NM_001700.3	AZU1	0.01	−1.13	−2.43	PM; ID
NM_004772.1	C5orf13	0.01	−2.08	−2.41	unclassified
NM_015166.2	MLC1	0.01	−0.69	−2.41	unclassified
NM_002163.2	IRF8	0.02	−1.92	−2.29	NM; ID;O
NM_005248.1	FGR	0.01	1.40	3.02	CM; PM; ST; ID; DP; CC; CP; O
NM_019058.2	DDIT4	0.03	1.88	3.03	unclassified
NM_000903.2	NQO1	0.01	2.13	3.06	unclassified
NM_022718.2	MMP25	0.01	1.63	3.18	PM
NM_005980.2	S100P	0.01	2.29	3.43	unclassified
NM_000591.1	CD14	0.01	0.65	3.44	ID
NM_012387.1	PADI4	0.01	1.48	3.62	PM
NM_015991.1	C1QA	0.01	3.56	3.68	ID
NM_000584.2	IL8	0.02	2.99	3.88	ST; ID; DP; CP; CS
NM_002982.3	CCL2	0.02	1.72	4.17	ST; ID

Values represent fold changes on $\log_2$ scale compared with control groups. CC, Cell cycle; CM, Carbohydrate metabolism; CP, Cell proliferation and differentiation; CS, Cell structure and motility; DP, Developmental processes; ID, Immunity & defense; NM, Nucleoside, nucleotide and nucleic acid metabolism; O, Oncogenesis; PM, Protein metabolism & modification; ST, Signal transduction.

A
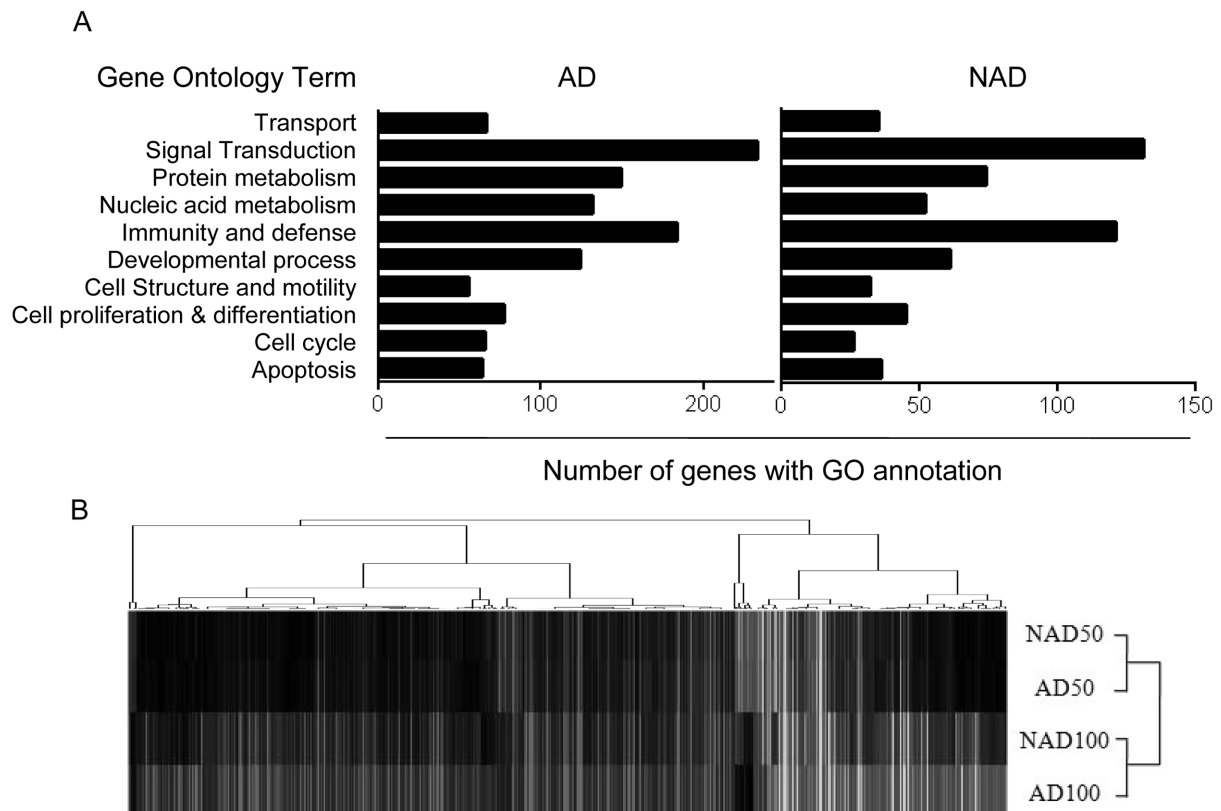
Fig. 3. Classification of gene function and hierarchical cluster analysis of differentially expressed genes. (A) The data of altered genes from exposure to AD-X or NAD-X in HL-60 cells were analyzed using Panther database (http://www.pantherdb.org). Representative biological processes are indicated in each group. (B) The analysis was performed on 587 genes obtained by adjusting the data using the Benjamini–Hochberg multiple test correction with a twofold cutoff. Red and green colors in the matrix indicate relative gene induction and repression, respectively. The dendrogram groups genes according to overall similarities in the gene expression profile.

after 24 h incubation with 50 or 100 μg/ml AD-X and NAD-X. Illumina gene expression arrays containing more than 24,000 oligonucleotide probes were used in triplicate control- and sample-treated HL60 cells. Technical replicates had a very high reproducibility with correlation coefficients of 0.92. One-way ANOVA ($p < 0.05$) and Benjamini-Hochberg data correction identified 573 AD-responsive (Supplementary Data 1) and 297 NAD-responsive genes (Supplementary Data 2). Table 2 and 3 show the top 10 up- and down-regulated genes by AD-X and NAD-X treatment, respectively. The degree of overlap in differentially expressed genes shown in the Venn diagram (Fig. 2B) indicates the existence of 283 overlapping genes between the AD-X and NAD-X treatments (Supplementary Data 3).

Functional classification of AD-X- and NAD-X-responsive genes. Functional categorization of the data was performed using the annotation information in the PANTHER database for ontology. AD-X-induced changes in expression of genes are involved in a variety of biological processes. The largest group of genes included those associated with signal transduction, while genes for immunity and

defense, protein metabolism and modification, and developmental processes were the next most abundant annotation groups (Fig. 3A). Tree analysis of the genes classified patterns of relative responses for all treatment conditions with respect to controls. The same dose groups, regardless whether given AD-X or NAD-X treatments, were in the same node, indicating a stronger dose effect in our experimental design (Fig. 3B).

Validation of gene expression in HL60 cells by Q-PCR. Q-PCR was used to verify the microarray data collected in this study. To compare the results directly, we used RNA from the same cells used for microarray hybridization. Mean fold changes of all samples from identically treated cells versus time-matched vehicle controls were compared between microarray and Q-PCR. We selected genes on the basis of the magnitude and direction (+/−) of gene expression from the AD-X 100 group; the gene expression changes of the 24 h samples are summarized in Table 4. From 10 genes selected for Q-PCR analysis, the expression of two genes differed from the microarray results. However, in most cases, a good correlation was observed between the

Table 4. Quantitative real-time PCR validation of selected genes from microarray data in AD-X 100 group

Gene	Microarray	qRT-PCR
AZU1	−3.05 ± 0.01	−2.20 ± 0.10
RP11-529I10.4	−1.18 ± 0.03	−0.99 ± 0.73
NUDT1	−1.17 ± 0.01	−0.72 ± 0.21
RABEPK	−1.11 ± 0.03	−1.34 ± 0.79
ARMET	−0.30 ± 0.07	−0.06 ± 0.18
FLJ10081	0.25 ± 0.04	−0.50 ± 0.04
CSTB	1.46 ± 0.01	1.87 ± 0.93
CD55	2.36 ± 0.06	1.40 ± 0.02
DDIT4	3.41 ± 0.07	5.69 ± 0.40

Data are expressed as fold-changes in a log2 scale compared to the control groups.
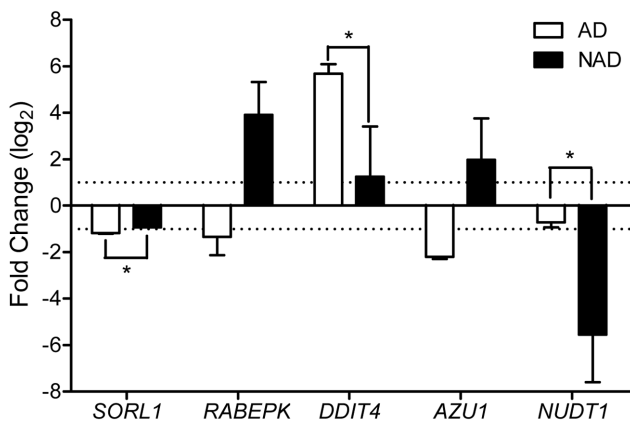
Fig. 4. Fold induction or repression of selected biomarker genes in HL-60 cells exposed to AD-X or NAD-X. The expression level of each gene was assessed by Q-PCR and normalized against GAPDH. Data are expressed as fold changes in a log2 scale compared to the corresponding control groups. Statistically significant differences between the two groups are indicated by an asterisk (*$p < 0.05$).

microarray and Q-PCR data (Table 4).

Identification of potential biomarkers. To identify potential biomarkers for AD exposure from the whole genes expressed differentially, we selected genes showing differential expression patterns following AD-X treatment compared to NAD-X treatment. We compared mean fold changes of all samples from AD-X- and NAD-X-treated cells versus time-matched vehicle controls. The expression patterns of five genes including *SORL1, RABEPK, DDIT4, AZU1,* and *NUDT1* differed significantly between the two groups (Fig. 4).

DISCUSSION

Growing evidence indicates that AD events are very closely associated with air pollution in the East Asian

region, which adversely impacts the health of the exposed population (Liu *et al.*, 2006; Kim *et al.*, 2008). AD aggravates respiratory symptoms and peak expiratory flow in children with mild asthma and increases cardiopulmonary emergency visits (Chan *et al.*, 2008; Yoo *et al.*, 2008). Consequently, a strong correlation is observed between the dust events and deaths from cardiovascular and respiratory causes (Kwon *et al.*, 2002). Several reasons exist for the adverse health effects caused by AD: the fine dust particle per se and the toxic chemicals adsorbed during long-range transport through the heavily polluted region of western China or in the highly contaminated urban areas are the major contributors. We recently analyzed the properties of AD and the toxic chemical components in AD collected in the source region (Inner Mongolia, China) and in the long-range transport region, including Beijing and Seoul, as highly polluted urban areas, and Cheju as a relatively clear rural area. Our unpublished data reveal higher levels of toxic heavy metals including lead, arsenic, chromium, and mercury. Higher levels of polycyclic aromatic hydrocarbons (PAHs) were also detected in dust samples from Seoul and Beijing than in those collected in the source region. Moreover, the concentrations of some PAHs were significantly higher in AD-X than NAD-X, indicating that these contaminants had been adsorbed during transport (Supplementary Data 4). Therefore, the toxic effects of the chemical mixture adsorbed to the AD particles warrant further study.

Multiple chemical exposures and their possible health effects have been important issues and concerns in the field of toxicology, especially in environmental toxicology (Altenburger *et al.*, 2004). However, the complex interactions of the chemicals with each other or with their molecular targets make understanding the toxicology of the chemical mixture difficult. The prediction of health effects from exposure to a chemical mixture is even more difficult (Yang, 1998). The mixture assessment performed by Finne *et al.* (2007), designed to address toxicity mediated by dissimilar modes of action, showed that the effects of the mixture were not predicted by the exposure to individual compounds. An important advantage of toxicogenomics including the amount of information, sensitivity of the results and thus applicability to low-dose exposure may offer improved assessment of the effects of chemical mixtures (Amin *et al.*, 2002). The development of biomarkers for exposure to chemical mixtures may be facilitated by use of this technology.

As shown in the Venn diagram, gene expression profiles of cells treated with AD-X and NAD-X exhibit considerable differences. This result is not unexpected considering the component analysis data regarding AD-X and NAD-X. Our unpublished data indicate that the concentrations of all nine PAHs analyzed in the study are higher in AD-X than in NAD-X. The concentration of benzo[*b*]fluoranthene was highest among the PAHs analyzed. The level of fluoranthene in NAD-X was below the detection limit, while that

in AD-X was 1700-fold higher (353 ng/g particles). Fluoranthene and benzo[b]fluoranthene are one of the 16 priority PAH compounds regulated by the Environmental Protection Agency that are produced by incomplete combustion of gasoline, coal, and oil and ubiquitously distributed in the environment. Fluoranthene is genotoxic and a suspected human carcinogen according to International Programme on Chemical Safety (IPCS, 1998). It is reported to cause lung and liver tumors in CD-1 mice (Wang and Busby, 1993) and apoptosis in T cells (Yamaguch et al., 1996). Benzo[b]fluoranthene induces DNA adducts and significant numbers of mouse lung adenomas (Mass et al., 1996). Among the genes differentially expressed by AD-X, genes coding for proteins involved in the bioactivation of PAHs (CYP1B1), DNA damage (DDIT4), DNA repair (NUDT1, NTHL1, DUT), protooncogene (FOS, KIT, SKP2), and angiogenesis (ENG) were significantly changed.

The use of gene biomarkers in environmental toxicology would be an efficient approach, especially in the risk assessment. The five genes that showed distinct expression pattern between AD-X and NAD-X treatment group may serve as potential biomarkers for AD exposure. DDIT4 (DNA-damage-inducible transcript 4), also known as RTP801, Dig2, or REDD1, is a novel stress response gene that is upregulated by a variety of extracellular stimuli such as DNA damage and oxidative stress induced by methyl methanesulfonate (Lin et al., 2005a), cisplatin (Kerley-Hamilton et al., 2005), and arsenite (Lin et al., 2005b). Considering the higher concentration of PAHs in AD-X than in NAD-X, the specific upregulation of DDIT4 in AD-X treated cells may provide a good marker for AD exposure.

The level of transcripts for NUDT1 (nucleoside diphosphate-linked moiety X-type motif 1) and SORL1 (sortilin-related receptor 1) were lowered by AD-X and NAD-X treatment in HL60 cells. Two independent studies demonstrated that the expression of NUDT1 and SORL1 were down-regulated in astrocyte gliomas, which account for more than 70% of all brain tumors (Jiang et al., 2006; MacDonald et al., 2007). The association of environmental pollution and the risk of gliomas was recently demonstrated. Subjects who lived in the region with the highest levels of petrochemical air pollution had a significantly greater risk of developing brain cancer than the group living in the lowest polluted area (Liu et al., 2008). Although the risk factors contributing to the etiology of brain tumors remain largely unknown, epidemiologic studies demonstrate that environmental factors inducing various types of DNA damage may play role in the pathogenesis of these tumors (Bondy et al., 1996). Therefore, the genetic alterations of the genes involved in DNA repair to maintain genomic stability may contribute to the disease. The expression levels of RABEPK (Rab9 effector protein with kelch motifs) and AZU1 (azurocidin 1) were reduced by AD-X, but increased by NAD-X.

We document global gene expression profile in HL-60 cells exposed to AD-X and NAD-X, as determined on oligonucleotide microarray. To the best of our knowledge, global gene expression study using AD has not been performed yet. Although the mechanistic correlation connecting the changes in gene expression with the hazard caused by exposure to AD remains unclear, these genes may provide information in developing surrogate markers for AD exposure and/or toxicity.

REFERENCES

Altenburger, R., Walter, H. and Grote, M. (2004). What contributes to the combined effect of a complex mixture? Environ. Sci. Technol., **38**, 6353-6362.

Amin, R.P., Hamadeh, H.K., Bushel, P.R., Bennett, L., Afshari, C.A. and Paules, R.S. (2002). Genomic interrogation of mechanism(s) underlying cellular responses to toxicants. Toxicology, **181-182**, 555-563.

Bondy, M.L., Kyritsis, A.P., Gu, J., de Andrade, M., Cunningham, J., Levin, V.A., Bruner, J.M. and Wei, Q. (1996). Mutagen sensitivity and risk of gliomas: a case-control analysis. Cancer Res., **56**, 1484-1486.

Chan, C.C., Chuang, K.J., Chen, W.J., Chang, W.T., Lee, C.T. and Peng, C.M. (2008). Increasing cardiopulmonary emergency visits by long-range transported Asian dust storms in Taiwan. Environ. Res., **106**, 393-400.

Chun, Y., Lim, J.Y. and Choi, B.C. (2003). The features of aerosol in seoul by asian dust and haze during springtime from 1998 to 2002. J. Kor. Meteorol. Soc., **39**, 459-474.

Finne, E.F., Cooper, G.A., Koop, B.F., Hylland, K. and Tollefsen, K.E. (2007). Toxicogenomic responses in rainbow trout (Oncorhynchus mykiss) hepatocytes exposed to model chemicals and a synthetic mixture. Aquat. Toxicol., **81**, 293-303.

Forrest, M.S., Lan, Q., Hubbard, A.E., Zhang, L., Vermeulen, R., Zhao, X., Li, G., Wu, Y.Y., Shen, M., Yin, S., Chanock, S.J., Rothman, N. and Smith, M.T. (2005). Discovery of novel biomarkers by microarray analysis of peripheral blood mononuclear cell gene expression in benzene-exposed workers. Environ. Health Perspect., **113**, 801-807.

Han, J.S., Moon, K.J., Ahn, J.Y., Hong, Y.D., Kim, Y.J., Ryu, S.Y., Cliff, S.S. and Cahill, T.A. (2004). Characteristics of ion components and trace elements of Fine Particles at Gosan, Korea in Spring time from 2001 to 2002. Environ. Monit. Assess., **92**, 73-93.

Husar, R.B., Tratt, D.M., Schichtel, B.A., Falke, S.R., Li, F., Jaffe, D., GassÓ, S., Gill, T., Laulainen, N.S., Lu, F., Reheis, M.C., Chun, Y., Westphal, D., Holben, B.N., Gueymard, C., McKendry, I., Kuring, N., Feldman, G.C., McClain, C., Frouin, R.J., Merrill, J., DuBois, D., Vignola, F., Murayama, T., Nickovic, S., Wilson, W.E., Sassen, K., Sugimoto, N. and Malm, W.C. (2001). Asian dust events of April 1998. J. Geophys. Res., **106**, 18316-18330.

IPCS (1998). Environmental health criteria 202: selected non-heterocyclic polycyclic aromatic hydrocarbons. World Health Organization (WHO), International Programme on Chemical Safety, Lyon, France.

Kerley-Hamilton, J.S., Pike, A.M., Li, N., Direnzo, J. and Spinella, M.J. (2005). A p53-dominant transcriptional response

to cisplatin in testicular germ cell tumor-derived human embryonal carcinoma. *Oncogene*, **24**, 6090-6100.

Kim, W., Doh, S.J., Yu, Y. and Lee, M. (2008). Role of Chinese wind-blown dust in enhancing environmental pollution in metropolitan Seoul. *Environ. Pollut.*, **153**, 333-341.

Kwon, H.J., Cho, S.H., Chun, Y., Legarde, F. and Pershagen, G. (2002). Effects of the Asian Dust Effects of the Asian Dust Events on Daily Mortality in Seoul, Korea. *Environ. Res.*, **90**, 1-5.

Li, G.Y., Lee, H.Y., Shin, H.S., Kim, H.Y., Lim, C.H. and Lee, B.H. (2007). Identification of gene markers for evaluation of exposure to formaldehyde in human. *Environ. Health Perspect.*, **115**, 1460-1466.

Lin, L., Qian, Y., Shi, X. and Chen, Y. (2005a). Induction of a cell stress response gene RTP801 by DNA damaging agent methyl methanesulfonate through CCAAT/enhancer binding protein. *Biochemistry*, **44**, 3909-3914.

Lin, L., Stringfield, T.M., Shi, X. and Chen, Y. (2005b). Arsenite induces a cell stress-response gene, RTP801, through reactive oxygen species and transcription factors Elk-1 and CCAAT/enhancer-binding protein. *Biochem. J.*, **392**, 93-102.

Liu, C.C., Chen, C.C., Wu, T.N. and Yang, C.Y. (2008). Association of brain cancer with residential exposure to petrochemical air pollution in Taiwan. *J. Toxicol. Environ. Health A*, **71**, 310-314.

Liu, C.M., Young, C.Y. and Lee, Y.C. (2006). Influence of Asian dust storms on air quality in Taiwan. *Sci. Tot. Environ.*, **368**, 884-897.

Mass, M.J., Abu-Shakra, A., Roop, B.C., Nelson, G., Galati, A.J., Stoner, G.D., Nesnow, S. and Ross, J.A. (1996). Benzo[b]fluoranthene: tumorigenicity in strain A/J mouse lungs, DNA adducts and mutations in the Ki-ras oncogene. *Carcinogenesis*, **17**, 1701-1704.

Mohr, S. and Liew, C.C. (2007). The peripheral-blood transcriptome: new insights into disease and risk assessment. *Trends Mol. Med.*, **13**, 422-432.

Park, E.J., Kim, D.S. and Park, K. (2008).Monitoring of ambient particles and heavy metals in a residential area of Seoul, Korea. *Environ. Monit. Assess.*, **137**, 441-449.

Parrington, J.R., Zoller, W.H. and Aras, N.K. (1983). Asian dust: Seasonal transport to the Hwaiian islands. *Science*, **220**, 195-197.

Taylor, D.A. (2002). Dust in the wind. *Environ. Health Perspect.*, **110**, A80-A87.

Wang, J.S. and Busby, W.F. Jr. (1993). Induction of lung and liver tumors by fluoranthene in a preweanling CD-1 mouse bioassay, *Carcinogenesis*, **14**, 1871-1874.

Yamaguchi, K., Near, R., Shneider, A., Cui, H., Ju, S.T. and Sherr, D.H. (1996). Fluoranthene-induced apoptosis in murine T cell hybridomas is independent of the aromatic hydrocarbon receptor. *Toxicol. Appl. Pharmacol.*, **139**, 144-152.

Yang, R.S.H. (1998). Some critical issues and concerns related to research advances on the toxicology of chemical mixture. *Environ. Health Perspect.*, **106**, 1059-1063.

Yoo, Y., Choung, J.T., Yu, J., Kim, D.K. and Koh, Y.Y. (2008). Acute effects of Asian dust events on respiratory symptoms and peak expiratory flow in children with mild asthma. *J. Kor. Med. Sci.*, **23**, 66-71.